

Structure and Properties of Murine and Human Dentin

Stefan Habelitz, Shabnam Zartoshtimanesh, Mehdi Balooch, Sally J. Marshall, Grayson W. Marshall, and *Pamela K. DenBesten,
Department of Preventive and Restorative Dental Sciences, *Department of Orofacial Sciences,
University of California, 707 Parnassus Ave., San Francisco, CA 94143-0758, USA

ABSTRACT

Mice are commonly considered the model mammal for many biomedical studies. In this work, mouse and human dentin were compared to specify structural and mechanical differences to establish a baseline for comparison of dental tissues between these species. Atomic force microscopy revealed tubules of about 1.0 to 1.6 μm in diameter as the main structural feature in dentin of both species. Nanoindentation yielded the elastic modulus about 15% lower in murine intertubular dentin while the hardness was almost equal. Dynamic stiffness mapping confirmed the lower elastic properties and also revealed that the peritubular region of increased mineralization around tubules is drastically reduced or maybe absent in murine dentin of this age. This study suggests that structural and mechanical differences need to be considered when murine dentin is used as a model system.

INTRODUCTION

Advances in biotechnology facilitated the design of mice with transgenic or deleted genes with the goal to elucidate the functions of various genes in the development, biology, pathology, structure, composition of various tissues and organs[1]. Research on mineralized tissues relies heavily on the use of mouse-models. An important issue for decades has been the assessment of the quality of bone, in particular with respect to osteoporosis and other bone diseases that affect the strength of the mineralized tissues[2-4]. Recent studies suggest that bone strength is not only a function of mass, but also related to local properties and concentrations of its component, like matrix proteins and apatite mineral as well as to the hierarchical structural design with these components as building blocks[5, 6]. Therefore, research on mineralized tissue requires a detailed analysis of microstructure and properties to give a more complete picture of the effect of a defective or altered gene or other factors studied through the mouse model. Mice teeth are of particular interest, since at least the incisors erupt continuously and therefore provide easy access to all stages of dental development in a single tooth, while molars provide insight into a mineralized tissue that remains unaltered after its development and does not undergo remodelling. Research on mice teeth has contributed significant knowledge in gene expression and function in amelogenesis and towards the etiology and pathology of genetic defects[7-9]. While these studies primarily focused on the biology, biochemistry and morphology of dental tissues, recent studies have pointed out the importance of a broader spectrum of criteria including micro- and nanostructure and nanomechanics to quantitatively distinguish between phenotypes[10, 11]. The aim of this study was to create a baseline for a mouse wildtype dentin phenotype based on microstructure and mechanical properties and to indicate differences between murine and human specimens. Atomic force microscopy, nanoindentation and elastic modulus mapping have been used to elucidate structural and physical similarities and dissimilarities between the dentin in these species.

EXPERIMENTAL DETAILS

Human third molars ($n = 5$) were extracted as part of a dental treatment and sterilized by gamma-radiation. Mice tooth samples were obtained from 2 months old mice by removing the mandibles ($n = 5$) and embedding them in epoxy-resin. Both, human and murine specimens were polished with a series of silica papers to the center of the midcoronal dentin and subsequently polished with a series of diamond pastes with a final grit size of $0.25 \mu\text{m}$. Specimens were carefully rinsed with deionized water and dried in air for at least one hour before evaluation. Five first molars were studied from mice and compared to five human third molars. Atomic force microscopy (AFM) (Digital Instrument, Nanoscope III, Santa Barbara, CA) with the standard head replaced by a transducer (Triboscope, Hysitron, Minneapolis, MN) with a diamond nanoindenter (Berkovich) was used for imaging and nanoindentation. The tip area function of the indenter was determined from measurements on fused silica ($E = 69.6 \text{ GPa}$). A maximum load of $500 \mu\text{N}$ was applied using a trapezoidal load-function with 3 sec. duration for each segment. Average values were obtained from a total of 100 measurements for each species. Dynamic stiffness measurements to create elastic modulus maps of dentin surfaces, used a cube-corner diamond indenter of calibrated shape in the oscillating mode, as described earlier [12]. Using a dual-channel lock-in amplifier, phase angle and amplitude changes could be recorded. Applying a model scheme including two Voigt elements, loss (E_{loss}) and storage (E_{store}) modulus were calculated, as described elsewhere [12]. Since E_{loss} contributed only minimal to the elastic deformation and was less than 5% of E_{store} , values for the elastic modulus (E) reported here reflect E_{store} only. Elastic modulus maps consist of 256 points of measurement for fast and slow scan axis. For $50 \mu\text{m}$ scan size, the pixel size was about 200 nm . Analysis of line plots of moduli along the x-axis were used to compare between samples.

RESULTS

AFM-imaging of human and murine dentin revealed dentin tubules of about $1.0 - 1.6 \mu\text{m}$ in diameter, as shown in Figure 1. The tubule density varied with location and increased towards the pulp. In the human specimen a thin rim of peritubular dentin (about $1 \mu\text{m}$) surrounded each tubule (Fig. 1a), while murine dentin exhibited no or very little of such zone (Fig.1b). Figures 2a and b, are elastic modulus maps obtained at the same location as the height-mode images of

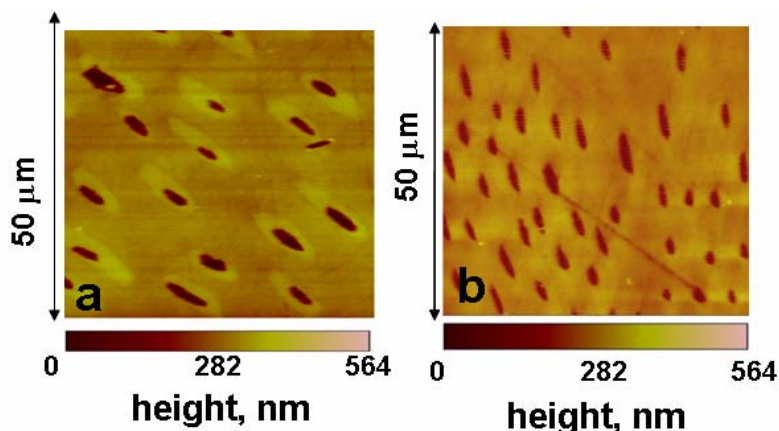


Figure 1: AFM height-mode image of a) human dentin and b) murine dentin.

Figure 1. These images reveal modulus changes in the specimens and show a significant increase of the modulus around the tubules in human dentin. In contrast, no or only a minor increase in modulus around tubules was observed in murine dentin.

Profiles of elastic moduli along the lines shown on the images in Figure 2 are plotted in Figure 3. The modulus of the intertubular dentin varied between 19 and 25 GPa for both species. The peritubular area in human dentin reached modulus values of up to 45 GPa, as shown in Figure 3a.

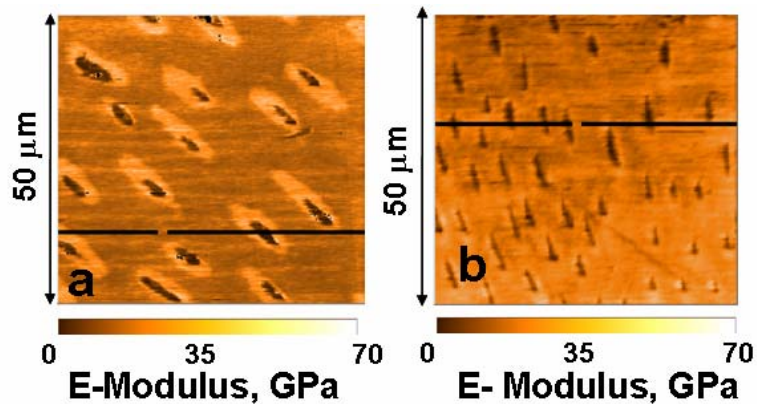


Figure 2: Elastic modulus map of a) human dentin and b) murine dentin obtained by dynamic stiffness measurements.

Discrete nanoindentations, twenty indents per sample, were placed on the intertubular dentin and an average modulus and hardness calculated. The mechanical properties of murine dentin were lower than those of human dentin, as shown in table 1. However, only the elastic modulus was significantly (T-test, $p < 0.05$) different.

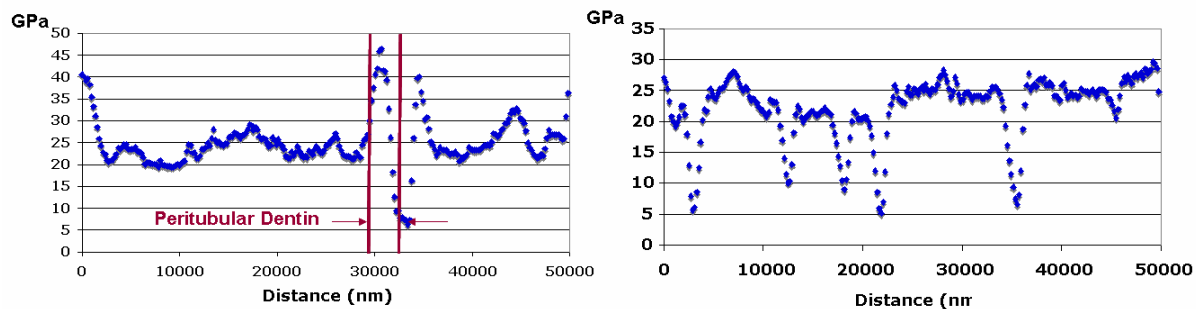


Figure 3: Plots of elastic moduli along the line shown in Figure 2 of a) human dentin and b) murine dentin. The strong increase of E around the tubules indicates the presence of a highly mineralized layer.

Table 1: Comparison of mechanical properties of human and murine intertubular dentin obtained by nanoindentation.

| | E-modulus (GPa) | Hardness (GPa) |
|------------------|-----------------|-----------------|
| Human | 24.0 ± 2.6 | 0.85 ± 0.12 |
| Mouse | 20.0 ± 2.4 | 0.83 ± 0.17 |
| P-value (t-test) | < 0.01 | 0.2 |

DISCUSSION

This paper compared the microstructure and the nanomechanical properties of human and murine dentin using AFM-based techniques. The presence of tubules, as rudiments of the odontoblast pathway during dentinogenesis was confirmed in both species. Imaging with the AFM and more clearly dynamic stiffness measurements revealed the presence of a rim of higher mineralization around the tubules in human dentin. This peritubular dentin reached a modulus of up to 45 GPa. It is thus between the values of intertubular dentin (20-24 GPa) and enamel (75-100 GPa) and most likely contains an intermediate amount of mineral. Interestingly peritubular dentin was not clearly identified in murine dentin and maybe absent at this young age of dentin. This observation supports the hypothesis that a zone of higher mineralization forms over time in the tubule walls as a process of apatite precipitation from the saturated pulpal fluid. Thus peritubular dentin may not be induced by specific biological factors. This hypothesis is also reinforced by the observation that peritubular size is increased in dentin from geriatric populations [13]. However, this increase occurs on the expense of the tubule lumen that can be filled completely with mineral in root dentin from this population. A comparison with dentin from older mice is aspired. Furthermore, the elastic properties of murine dentin appeared to be decreased compared to the human counterpart, suggesting a lower degree of mineralization in mice teeth.

CONCLUSIONS

Mice and human dentin show significant differences in their structure and properties. These differences need to be considered when studies on mice are applied in a model-system.

ACKNOWLEDGEMENT

This research was supported by the National Institutes of Health/National Institute of Dental and Craniofacial Research, Grants P01DE09859 and R21-DE015416.

REFERENCES

1. Hasty, P., J. Campisi, J. Hoeijmakers, H. van Steeg, and J. Vijg, *Science*. **299**, 1355-9 (2003).
2. Filvaroff, E., A. Erlebacher, J. Ye, S.E. Gitelman, J. Lotz, M. Heilmann, and R. Derynck, *Development*. **126**, 4267-79 (1999).
3. Kozloff, K.M., A. Carden, C. Bergwitz, A. Forlino, T.E. Uveges, M.D. Morris, J.C. Marini, and S.A. Goldstein, *J Bone Miner Res*. **19**, 614-22 (2004).
4. Lane, N.E., W. Yao, J.H. Kinney, G. Modin, M. Balooch, and T.J. Wronski, *J Bone Miner Res*. **18**, 2105-15 (2003).
5. van der Meulen, M.C., K.J. Jepsen, and B. Mikic, *Bone*. **29**, 101-4 (2001).
6. Nalla, R.K., J.J. Kruzic, and R.O. Ritchie, *Bone*. **34**, 790-8 (2004).
7. Dunglas, C., D. Septier, M.L. Paine, D.H. Zhu, M.L. Snead, and M. Goldberg, *Calcif Tissue Int*. **71**, 155-66. (2002).
8. DenBesten, P.K., D. Machule, R. Gallagher, G.W. Marshall, Jr., C. Mathews, and E. Filvaroff, *Adv Dent Res*. **15**, 39-41 (2001).

9. Gibson, C.W., Z.A. Yuan, B. Hall, G. Longenecker, E. Chen, T. Thyagarajan, T. Sreenath, J.T. Wright, S. Decker, R. Piddington, G. Harrison, and A.B. Kulkarni, *J. Biol. Chem.* **276**, 31871-5. (2001).
10. Paine, M.L., D.H. Zhu, W. Luo, P. Bringas, Jr., M. Goldberg, S.N. White, Y.P. Lei, M. Sarikaya, H.K. Fong, and M.L. Snead, *J Struct Biol.* **132**, 191-200. (2000).
11. Fong, H., S.N. White, M.L. Paine, W. Luo, M.L. Snead, and M. Sarikaya, *J Bone Miner Res.* **18**, 2052-9 (2003).
12. Balooch, G., G.W. Marshall, S.J. Marshall, O.L. Warren, S.A. Asif, and M. Balooch, *J Biomech.* **37**, 1223-32 (2004).
13. TenCate, A. R. *Oral Histology: development, structure and function.* 5th Edition, St. Louis, Mosby, (p.158-159) 1998.